JOURNAL OF QUATERNARY SCIENCE (2018) **33**(6) 713–720 ISSN 0267-8179. DOI: 10.1002/jqs.3047

JQS Journal of Quaternary Science QRA Quaternary Research Association

Ostracod-based reconstruction of Late Quaternary lake level changes within the Tangra Yumco lake system (southern Tibetan Plateau)

M. ALIVERNINI,[1]* L. G. AKITA,[2] M. AHLBORN,[3] N. BÖRNER,[4] T. HABERZETTL,[5] T. KASPER,[5] B. PLESSEN,[3] P. PENG,[6] A. SCHWALB,[4] J. WANG[6] and P. FRENZEL[1]

[1]Institut für Geowissenschaften, Friedrich-Schiller-Universität, Jena, Germany
[2]Department of Marine and Fisheries Sciences, University of Ghana, Accra, Ghana
[3]German Research Center for Geosciences, Helmholtz-Center Potsdam, Potsdam, Germany
[4]Institut für Geosysteme und Bioindikation, Technische Universität Braunschweig, Germany
[5]Institut für Geographie, Friedrich-Schiller-Universität Jena, Jena, Germany
[6]Institute of Tibetan Plateau Research, Chinese Academy of Sciences, Beijing, China

Received 13 February 2018; Revised 17 April 2018; Accepted 29 April 2018

ABSTRACT: Tangra Yumco, a large saline lake located in the central–southern part of the Tibetan Plateau, lies in a hydrologically closed basin and is part of a cascade lake system including Tangqung Co, Tangra Yumco and Xuru Co. The extension and position of this lake system makes it valuable for reconstructing palaeoclimatic variations through the lake history and to compare both with the adjacent lake systems. We reconstructed Late Quaternary lake level changes based on data from two lacustrine sediment cores. A micropalaeontological analysis focusing on Ostracoda was carried out combined with dating (^{14}C, ^{210}Pb, ^{137}Cs), sedimentology and stable isotope data from bulk sediment. Ostracod analysis involves the quantitative documentation of associations. An ostracod-based transfer function for specific conductivity was applied to assess and refine lake level changes and to compare the results with other lake level reconstructions from the Tibetan Plateau for evaluating inter-regional climatic patterns. Seven ostracod species were detected, with *Leucocytherella sinensis* dominating the associations followed by *Leucocythere*? *dorsotuberosa*, *Limnocythere inopinata* and *Tonnacypris gyirongensis*. *Fabaeformiscandona gyirongensis*, *Candona candida* and *Candona xizangensis* were found in only a few samples and at low percentages. The synthesis of ostracod-based environmental reconstruction and chronology for samples from Tangra Yumco reveals the evolution of the lake system during the past 17 ka. A low lake level around 17 cal ka BP is followed by a recovering until the reaching of a high stand around 8–9 cal ka BP. Subsequently, between 7.7 and 2.5 cal ka BP, it remained relatively stable with a subsequent short-living lowstand–highstand cycle at around 2 ka. Thereafter, the ostracod-based conductivity transfer function shows an increase of conductivity corresponding to a lake level rising phase at around 0.4 ka. The recorded changes are indicators of past climatic conditions and refine the palaeoclimatic models in this area.

KEYWORDS: conductivity; Late Quaternary; micropalaeontology; palaeoclimate; Tangra Yumco.

Introduction

In the last decade, several studies of lacustrine sediments from the Tibetan Plateau identified significant lake level changes during the Late Quaternary that are related to monsoon and westerlies variability (Mischke and Zhang, 2010; Kasper *et al.*, 2012; Günther *et al.*, 2013, 2015, 2016; Mishra *et al.*, 2015; Ahlborn *et al.*, 2016; Henkel *et al.*, 2016). Due to the role of this area as origin of many large rivers of south-eastern Asia, the climate variations in this area force environmental, social and economic consequences for millions of people and their better understanding is urgently needed to offer indications of future scenarios.

A multi-proxy approach, integrating chemical, physical and palaeontological data, was applied in this study to reconstruct the lake level variations of Tangra Yumco in detail. In such a context, ostracods have already been widely used as palaeoenvironmental indicators on the Tibetan Plateau (e.g. Mischke *et al.*, 2006; Frenzel *et al.*, 2010; Wrozyna *et al.*, 2010, 2012; Mischke, 2012; Ahlborn *et al.*, 2015; Akita *et al.*, 2015; Alivernini *et al.*, 2018). Palaeoecological applications of ostracod-based transfer functions have proven to be a useful tool to assess palaeoclimatic conditions (Mischke, 2012; Viehberg and Mesquita-Joanes, 2012). Such approaches have generally been used to reconstruct relative lake level changes on the Tibetan Plateau, identifying the timing of past moisture availability and evaporation intensity.

This work focuses on the lake Tangra Yumco, which is part of a cascade lake system including Tangqung Co, Tangra Yumco and Xuru Co (Fig. 1), located on the southern–central Tibetan Plateau. Tangra Yumco has been investigated in several studies in recent years to assess lake level changes during the Late Quaternary (Long *et al.*, 2012; Rades *et al.*, 2013; Miehe *et al.*, 2014; Ahlborn *et al.*, 2016, 2017; Günther *et al.*, 2016; Henkel *et al.*, 2016). Akita *et al.* (2016) provided a dataset of the ecology of recent Ostracoda of Tangra Yumco as a groundwork for palaeoecological applications. In Ahlborn *et al.* (2016) an analysis on surface samples was carried out and a lake level curve of Tangra Yumco was reconstructed. We compared these with the results of this study to have a continuous dataset to refine their results. For the present study, an 11.5-m-long piston core (31°13.93′N, 86°43.25′E, 217 m water depth) and a gravity core (31°15.15′N, 86°

*Correspondence: M. Alivernini, as above.
E-mail: mauro.alivernini@uni-jena.de

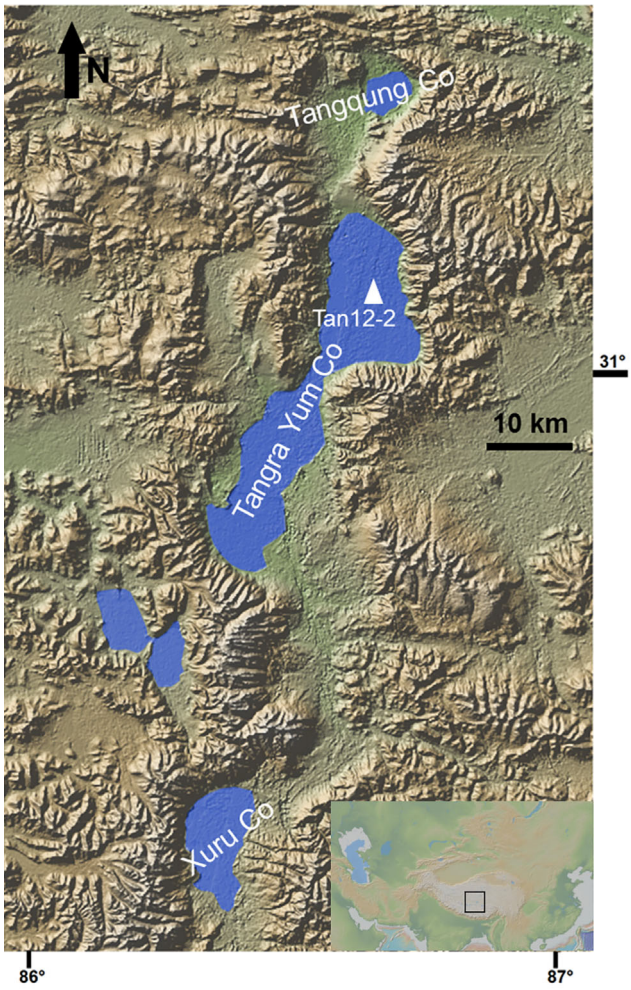

Figure 1. Location of the three studied lakes of the Tangra Yum Co lake system (with elevation, area and salinity): Tangqung Co (4475 m a.s.l.; 57 km^2; *ca.* 100‰), Tangra Yum Co (4595 m a.s.l.; 818 km^2; 8.3‰) and Xuru Co (4720 m a.s.l.; 206 km^2; 3.2‰). Source: www.geomapapp.org. Lake Monco Bunnyi was not part of the Tangra Yum Co lake system during the investigated time frame. The position of sediment core TAN12-2 is indicated by the white triangle.

43.37′E, 223 m water depth) located close-by were micropalaeontologically analysed, dated by ^{14}C, and for the piston core the resulting chronology was confirmed by palaeomagnetic secular variation stratigraphy (Haberzettl *et al.*, 2015; Henkel *et al.*, 2016).

Tangra Yumco together with other large lakes improves our understanding of hydrological system changes on the southern–central Tibetan Plateau and the varying monsoonal impact. Estimation of the specific conductivity is valuable tool in reconstructing lake level changes and switches from open to closed lake basins or vice versa, allowing a comparison with neighbouring lakes and other basins on the Tibetan Plateau.

This work aims (i) to reconstruct the Late Quaternary evolution of the Tangra Yumco lake system, by refining and integrating the work of several authors (Ahlborn *et al.*, 2016, 2017; Henkel *et al.*, 2016), (ii) to assess possible scenarios of the interactions between the basins of the Tangra Yumco system during the past 17 ka using an ostracod-based conductivity reconstruction to discriminate climatic and hydrographic effects and (iii) to contribute to a holistic picture by comparing with other lakes in order to detect climate shifts along an east–west transect on the southern Tibetan Plateau during the Late Quaternary.

Study area

Tangra Yumco (30°45′–31°22′N, 86°23′–89°49′E; Fig. 1) is a terminal lake located on the central-southern Tibetan Plateau at an elevation of 4545 m a.s.l. (Rades *et al.*, 2013) with a catchment size of 8219 km^2 and a salinity of 8.3‰ (Long *et al.*, 2012). Tangra Yumco is the second deepest (230 m m) lake in China (Wang *et al.*, 2010) and third largest lake on the Tibetan Plateau. The population in the Tangra Yumco area is sparse and human impact is mainly restricted to pastoralism (Miehe *et al.*, 2014). Precipitation at Tangra Yumco is mainly dominated by the Indian summer monsoon originating from the south (Miehe *et al.*, 2014) and westerly winds during the winter months (Maussion *et al.*, 2014). Today, the lake system comprises three lakes: Tangra Yumco, Tangqung Co and Xuru Co located in a 300-km-long and 40-km-wide graben (Akita *et al.*, 2016). Tangra Yumco and adjoining lakes are covered with ice in winter but do not completely freeze in some years due to the high salinity of their waters (Kropáček *et al.*, 2013). The cold arid climate supports alpine meadow with *Kobresia* and steppe vegetation with *Artemisia* (Miehe *et al.*, 2014). Tangra Yumco is an endorheic lake formed by active tectonic movement in a north–south-trending graben (Zhu *et al.*, 2004; Kong *et al.*, 2011). Whereas the southern Tibetan Plateau is dominated by Palaeozoic–Mesozoic carbonate and clastic sedimentary rocks (Galy and France-Lanord, 1999), the flank of the rift of Tangra Yumco is mainly composed of volcanic rocks, granitoid intrusions and potassic lavas (Gao *et al.*, 2010). During the middle Pleistocene, the three water bodies formed one large lake and lacustrine deposits are well preserved between Tangqung Co and Tangra Yumco (Kong *et al.*, 2011). The three lakes are arranged as on a staircase, with Xuru Co seated at the highest position (4720 m a.s.l.) and the other basins subsequently lower. Tangra Yumco has two large rivers entering from the south-east and west but no outflow. Due to its terminal character, lake level variations of Tangra Yumco are mainly controlled by precipitation and the contribution of glacial meltwater is negligible (Biskop *et al.*, 2015). Quaternary palaeo-shorelines and lake terraces are located up to 200 m above the present-day lake level of Tangra Yumco (Rades *et al.*, 2013), indicating a Holocene shrinkage of a larger ancient lake (Long *et al.*, 2012; Liu *et al.*, 2013; Ahlborn *et al.*, 2017). The large lake was divided gradually into independent smaller water bodies during the Early and Late Holocene due to an extensive drop of water level (Zhang, 2000; Zhu *et al.*, 2004; Liu *et al.*, 2013). However, the presence of submerged lake level terraces (Akita *et al.*, 2015) indicates significantly lower lake levels in the past. Additionally, beach rocks formed by precipitation of secondary carbonates, Holocene stromatolites and tufa can be found in the northern part of the Tangqung Co catchment (Akita *et al.*, 2015).

Material and methods

Sedimentological analysis

The composite profile consists of the 1.62-m-long gravity core TAN 10/4 and the 11.5-m-long piston core TAN12-2 (Henkel *et al.*, 2016). The complete record with lamination of different thickness (sub-mm to cm) consists of interbedded silty sediments and blackish sandy layers (Fig. 2). The cores were subsequently sampled every centimetre. For further details, see Henkel *et al.* (2016). In Tangra Yumco radiocarbon dating on the cores yielded ages from 17.4 cal ka BP to today, for a total of 29 dated samples (Ahlborn *et al.*, 2017).

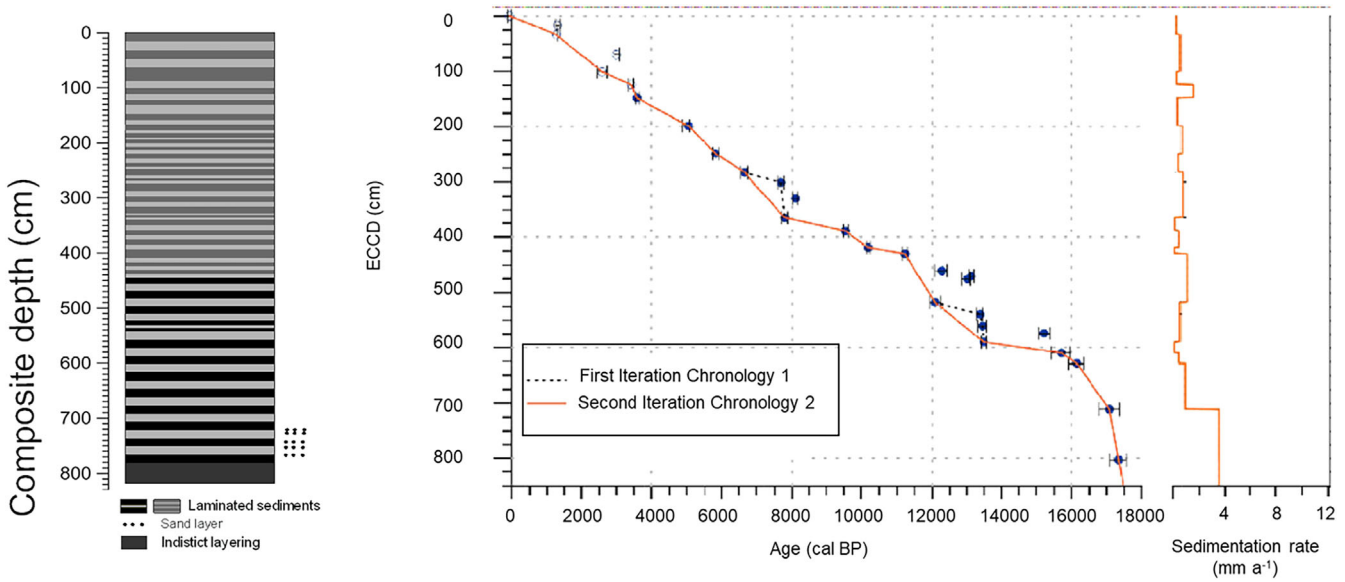

Figure 2. Composite profile (without turbiditic layers) of the two cores with age–depth model and sedimentation rates as published by Henkel *et al.* (2016).

Micropalaeontology

In total, 168 samples containing mostly disarticulated ostracod valves were taken every 10 cm, and shorter intervals if valves were not found within selected samples. The results from the pilot core TAN 10/4 (126 sub-samples) were integrated in the piston's core dataset to complete the record for the most recent past. Species percentages and total ostracod abundance were calculated. For ostracod abundance, juvenile and adult stages were counted separately. The adult/juvenile ratio was determined to assess water turbulence (Boomer *et al.*, 2009) and to check for possible removal of thinner juvenile valves by dissolution. Samples were treated with H_2O_2 (ca. 5% for about 1–3 h) and subsequently sieved with water through a 200-μm sieve to enrich the valves. In addition, the sieve residues were split into sub-samples using a microsplitter to perform a more indicative quantitative analysis with a large number of valves. Identification was mainly done with a low-power binocular microscope and occasionally supported by a scanning electron microscope as well as a Keyence Digital Microscope and the ostracods were classified on the basis of previous taxonomical works in this geographical area (e.g. Mischke, 2012; Wrozyna *et al.*, 2010). Valves were subsequently counted to 300–500 individuals for every sample. If the number of 50 valves in a single sample was not reached, the samples were combined with the subsequent samples to achieve the required minimum number of valves (>50), within 0.1-ka intervals. For a complete overview of the grouped samples and the ostracod species see the Supporting Information (https://doi.pangaea.de/10.1594/PANGAEA.890591).

An ostracod-based transfer function for the reconstruction of past conductivity values was applied (Peng *et al.*, 2016) to trace lake level and system changes. The modern training set of Peng *et al.* (2016) covers 34 lakes of the southern and western Tibetan Plateau with a total of 75 samples and conductivity ranging from 0.3 to 18 mS cm^{-1}. The program C2 (Juggins, 2003) and Weighted Averaging Partial Least Squares (WAPLS) regression were used (Mischke *et al.*, 2007; Guo *et al.*, 2016) to develop quantitative relationships between environmental variables and ostracod assemblages. The conductivity values were $\log_{10}$-transformed before calculation. The performance of the ostracod-based conductivity transfer function is indicated by a correlation of $R^2 = 0.77$ between observed and estimated values and an error (RMSEP) of 0.25 (Peng *et al.*, 2016).

Stable oxygen isotope analysis

For stable isotope analysis, the cores TAN 10/4 and TAN12-2 were sampled at intervals of 1 cm, and bulk sediment was freeze-dried and ground. The analysis of stable oxygen isotopes was carried out at Helmholtz-Zentrum Potsdam, Deutsches Geoforschungszentrum (GFZ), Germany, using a Finnigan GasBench-II with carbonate-option connected to a DELTAplus XL isotope ratio mass spectrometer (IRMS). Before analysis sediment samples were reacted with 100% H_3PO_4 at 75 °C for 60 min, and each sample was analysed nine-fold. Results are expressed in the standard delta notation in per mil relative to VPDB (Vienna Pee Dee Belemnite). Standardization was done using international reference materials IAEA-NBS18 and NBS19, as well as laboratory internal standards CO1 and C1 (calibrated against VPDB). Analytical precision was better than ± 0.07‰ for $\delta^{18}O$.

Results

Micropalaeontological analysis

The composite profile comprising the short and the long core covers about 18 ka. Total abundances vary between 32 and 602 valves g^{-1} with a mean value of 109 valves g^{-1} for both cores (Fig. 3). Most valves were disarticulated and juvenile valves were dominant. Ostracods were lacking in the oldest part of the core, *i.e.* between 18 and 17 cal ka BP. After this, *Limnocythere inopinata* (Baird, 1843) was dominant until *ca.* 16.0 cal ka BP and, from 16.0 to 12 cal ka BP *Leucocythere? dorsotuberosa* (Huang, 1982) became the most frequent species. Between *ca.* 12 and 10 cal ka bp, three dominant species were detected in different intervals. The most prominent species is the opportunistic *Leucocytherella sinensis* (Huang, 1982), which often occurs in association with *Leucocythere? dorsotuberosa*. *Fabaeformiscandona gyirongensis* (Huang, 1982) was prominent at around 10.1 cal ka BP. After this interval, *L.? dorsotuberosa* returned to be dominant until 5 cal ka BP. Concerning the final period, *Leucocytherella sinensis* and *L.? dorsotuberosa* were alternately dominating from 1.8 cal ka BP until today, but they are largely replaced by *L. inopinata* for the period between 1.8 cal ka BP and 400 bp

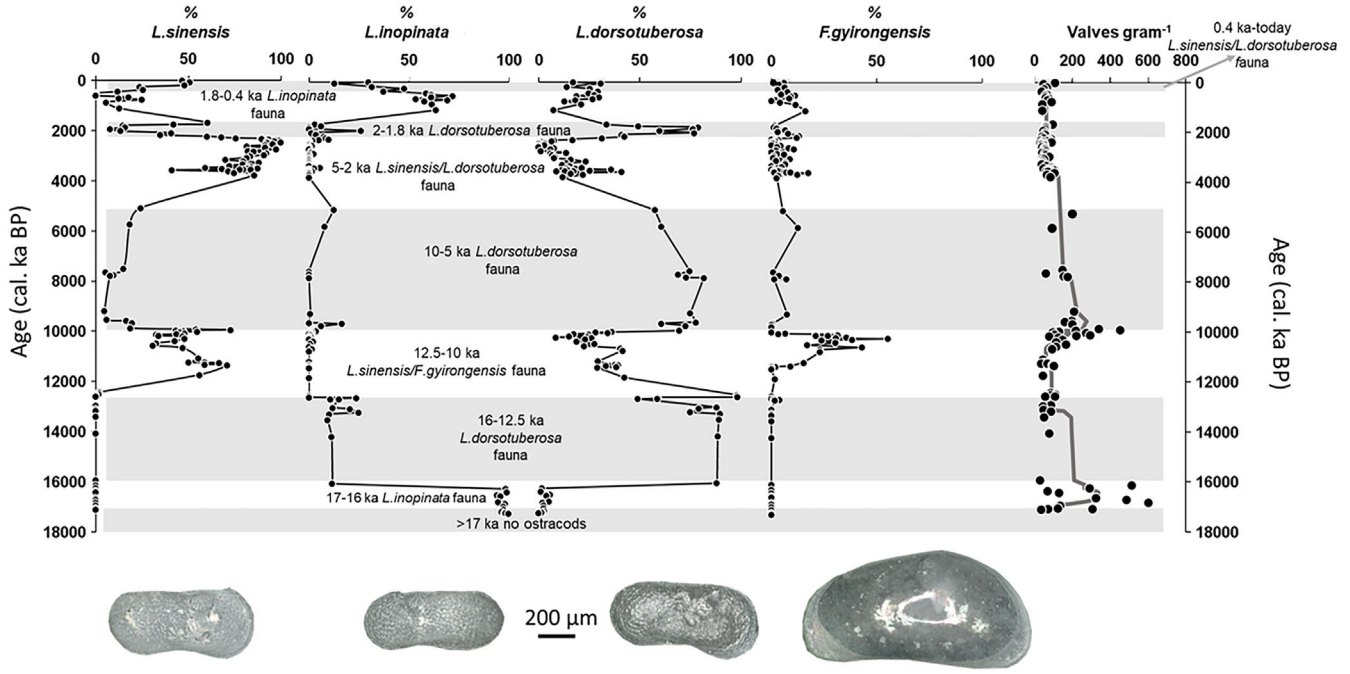

Figure 3. Relative abundances and valves/weight ratio of the ostracods. For relative abundances only the most abundant species were considered. From left to right, *L. sinensis* adult male, RV, ext., *L. inopinata* adult male, LV ext., *L.? dorsotuberosa* adult male, LV ext., *F. gyirongensis* adult female, RV, int.

cal a BP. *Candona xizangensis* (Huang, 1982), *Tonnacypris gyirongensis* (Yang, 1982) and *Candona candida* (O.F. Müller, 1776) were also found but in very small percentages along the cores. The relative abundances of the most abundant ostracods are shown in Fig. 3.

Conductivity reconstruction

The conductivity transfer function shows the highest value of 13.6 mS cm^{-1} close to the bottom of the composite core TAN12-2 at 17.1–16.1 cal ka BP (Fig. 4). Thereafter, the conductivity follows a general decreasing trend, reaching its minimum value (0.6 mS cm^{-1}) around 10.1 cal ka BP. Subsequently, conductivity increases again until 9.6 cal ka bp (3.3 mS cm^{-1}). Thereafter, values decrease until 1.7 cal ka BP, ranging between 2.8 and 1.2 mS cm^{-1} with the exception of a single peak of 4.3 mS cm^{-1} around 1.9 cal ka BP. For the last 1.1 ka, values range between 5.2 and 8.2 mS cm^{-1} and, close to the top of the core, are *ca.* 0.4 cal ka BP; today, conductivity generally shows a decrease, with values between 5.1 and 2.1 mS cm^{-1}.

Stable oxygen isotopes

The $\delta^{18}O$ record from Tangra Yumco shows high values at around 17.0 cal ka BP. After this there is a general decrease until about 11.0 cal ka BP. Thereafter the curve follows a positive trend towards higher values until about 0.4 cal ka BP, where a new negative trend until today was observed.

Discussion and interpretation

Lake level changes of the Tangra Yumco lake system

A possible explanation for the lack of ostracods between 18 and 17 cal ka BP could be high salinity as indicated by high $\delta^{18}O$ values of the bulk sediment (Fig. 4) and a high sedimentation rate due to a pronounced low lake level stand. This hypothesis is also supported by the reconstructed conditions of the lake level between 17 and 16 cal ka BP, with a dominance of *L. inopinata*. This species indicates a low lake level and meso- to polyhaline conditions in the southern part of the Tibetan Plateau (Akita *et al.*, 2016). At the same time *L.? dorsotuberosa* confirms the presence of a lacustrine water body. The maximum conductivity reached during this period is 13.6 mS cm^{-1}. Until about 12 cal ka BP, the dominance of *L.? dorsotuberosa* indicates a rising lake level (Akita *et al.*, 2016) with a correspondingly decreasing conductivity and negative $\delta^{18}O$ trend. Based on the increased relative abundance of *L. sinensis* and lower numbers of the deep water species *L.? dorsotuberosa*, there was a slight increase in water depth during this period, although the conductivity transfer function does not show a clear trend. This alternation could be due to temporary variations of the lake level or variations to the inflow/outflow of the system. The switch in dominance from *L.? dorsotuberosa* to the opportunistic *L. sinensis* and shallow-water taxon *L. inopinata* (Akita *et al.*, 2016) between 9.8 and 7.5 cal ka BP indicates a slow and progressive lowering of the lake level with a corresponding slight increase in conductivity. This trend is also confirmed by $\delta^{18}O$ analysis, indicating an enrichment in heavy ^{18}O isotopes within the sediments after 8.5 cal ka BP, which can be assumed to be directly related to the lake water, reflecting a decrease in effective moisture and thus a slow, long-term reduction in lake water volume typical of large terminal lakes (Leng and Marshall, 2004). These $\delta^{18}O$-based lake volume reconstructions are supported by a quantitative lake level reconstruction from Tangra Yumco based on optically stimulated luminescence (OSL) ages of exposed lacustrine sediments (Ahlborn *et al.*, 2016) showing a very similar pattern (Fig. 4).

During the period 7.5–3.7 cal ka BP the evolution of the lake could not be reconstructed based on the ostracod assemblage as only two samples dated to 5.7 and 5 cal ka BP are available. Nevertheless, the bulk sediment oxygen isotopes show a gradual increase, indicating a high but gradually falling lake level accompanied by slowly increasing conductivity.

For the last 3.7 cal ka BP, it is possible to distinguish four phases (Fig. 3). The first, with *L. sinensis* as the dominant species,

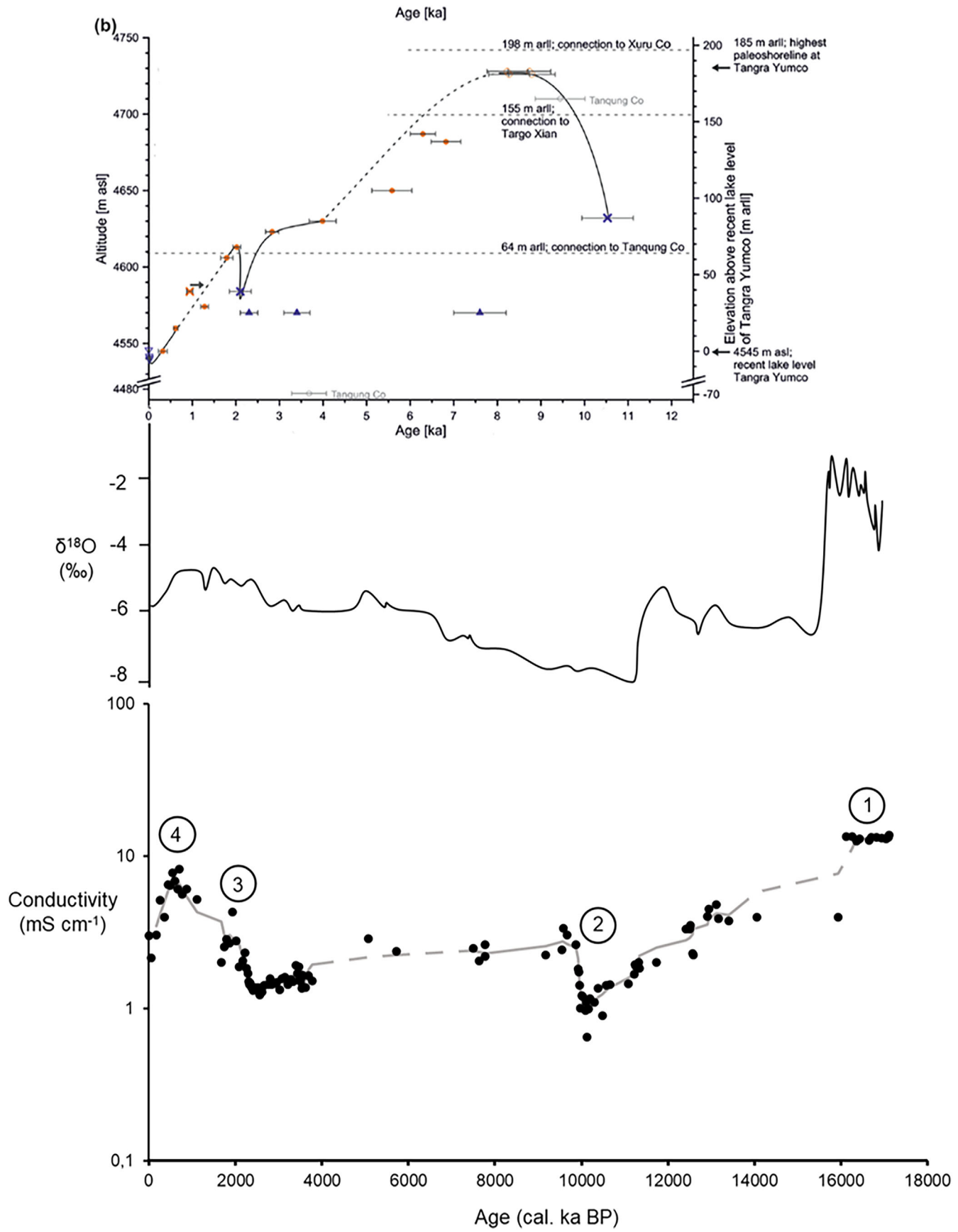

Figure 4. Comparison of the lake level curve of Ahlborn et al. (2016; upper diagram), changes in bulk $\delta^{18}O$ and ostracod-based conductivity estimation. The black points are calculated values and the grey line indicates the 5-point average (the broken line indicates uncertainties due to a lack of samples). In the oldest stage (1) at 17–10.5 ka cal BP, the conductivity decreases. (2) An increase is recorded, followed by a decrease, in contrast to Ahlborn *et al.*'s record. Good agreement with Ahlborn *et al.*'s (2016) curve is recognizable around 2 ka (3), and by the fast switch of decreasing and later increasing lake level reported in the conductivity curve. Subsequently (4), the two curves agree until 0.4 ka cal BP where the conductivity starts to decrease earlier than the rise of the lake assumed by Ahlborn *et al.* (2016).

indicates a relatively stable lake level with low conductivity and corresponding oligohaline conditions. Around 2 ca ka BP, a switch in dominance between *L. sinensis* and the two species *L.? dorsotuberosa* and *L. inopinata* suggests a fast lake level decline and a subsequent fast rise. The dominance of the halotolerant species *L. inopinata* between 1.1 and 0.2 cal ka BP indicates mesohaline conditions and a falling lake level. In the uppermost six samples, *L. sinensis* reappears, probably due to a recovery of the lake level as also confirmed by $\delta^{18}O$ analysis revealing a negative trend during this period.

Comparison with previous studies and regional comparison

Tangra Yumco sediments have already been investigated for palaeoecological and palaeoclimatic purposes in the recent years (Long *et al.*, 2012; Rades *et al.*, 2013; Miehe *et al.*, 2014; Ahlborn *et al.*, 2016, 2017; Akita *et al.*, 2016; Günther *et al.*, 2016; Henkel *et al.*, 2016). Ahlborn *et al.* (2016) reconstructed the lake level history based on OSL dating (Fig. 4) of massive carbonate banks in the catchment of Tangra Yumco integrating similar datasets from several authors (Kong *et al.*, 2011; Long *et al.*, 2012; Rades *et al.*, 2013, 2015). In addition of this, we match our micropalaeontological data with datasets presented by Ahlborn *et al.* (2017), who compared lithological and geochemical analysis on the cores of Tangra Yumco with similar records from other water bodies on the southern part of the Tibetan Plateau, and with the results of the $\delta^{18}O$ analysis data from Tangra Yumco. Regarding the whole system, neotectonics probably had only a minor role in the interaction between the lakes, given the dramatic lake level fluctuations and the relatively low impact of tectonics in this region (Armijo *et al.*, 1986).

Akita *et al.* (2016) demonstrated small and temporary water bodies were populated by different ostracod assemblages compated with large lakes, but the distribution of lacustrine ostracods is mainly driven by salinity. This observation was made by Mischke *et al.* (2007) as well and supports the reliability of ostracod-based conductivity transfer functions for lakes of the Tibetan Plateau.

The results show low conductivity values, probably related to a shallow lake level around 17 ka, also confirmed by Ahlborn *et al.* (2017). After this, merging of the lake Tangqung Co in Tangra Yumco, forming one large lake at around 10.5 cal ka BP, is recorded (Ahlborn *et al.*, 2016). Subsequently to this period, a highstand of 181–183 m above the present lake level is recorded and Tangra Yumco reached its highest elevation during the entire Holocene between 9 and 8 cal ka BP (Ahlborn *et al.*, 2016). A comparison of the lake level reconstruction of Ahlborn *et al.* (2016) with the ostracod-based conductivity of the present study shows a generally similar pattern, especially concerning the first phase of increasing lake level (10.5 cal ka BP) and the phase between 4 and 0.4 cal ka BP, where the lake level shows lowstand–highstand switches followed by a new decrease, before stabilizing. However, some differences are observed (Fig. 4). At about 10 cal ka BP, conductivity shows an increase, despite a postulated lake level rise. A possible explanation could be that before this event, Tangra Yumco was integrated to Tangqung Co with a decrease of conductivity due to overflowing into the latter. With a further rise of the lake Tangqung Co at about 10.2 ka, the latter reached the water level of Tangra Yumco, mixing with its more saline waters and leading to a subsequent increase in conductivity. The results indicate, at about 9.8 cal ka BP, a decrease in conductivity as result of the further rise of the lake level. The general lack of data for the period 7.5–3.7 cal ka BP for the ostracod dataset and for the OSL samples does not allow a more precise reconstruction, although a moderate trend of increasing conductivity is conceivable.

The documented conductivity reconstruction based on ostracods shows a rapid highstand–lowstand at around 2 cal ka BP (Fig. 4), documented also in the OSL-based reconstruction of Ahlborn *et al.* (2016). Although not shown in the isotope data, the slight increase is probably compounded by the short-term mixing with Tangqung Co water. So our proxy would show this minor variation best. In the youngest part of the record the conductivity increase is confirmed by the lake level trend documented by Ahlborn *et al.* (2016). After *ca.* 0.4 cal ka BP, decreasing conductivity, as suggested by the ostracod conductivity transfer function, is in contrast to a falling lake level indicated by the OSL-based reconstruction. However, this result agrees with the $\delta^{18}O$ ratio dataset from the same core where a negative trend of the isotopes for the

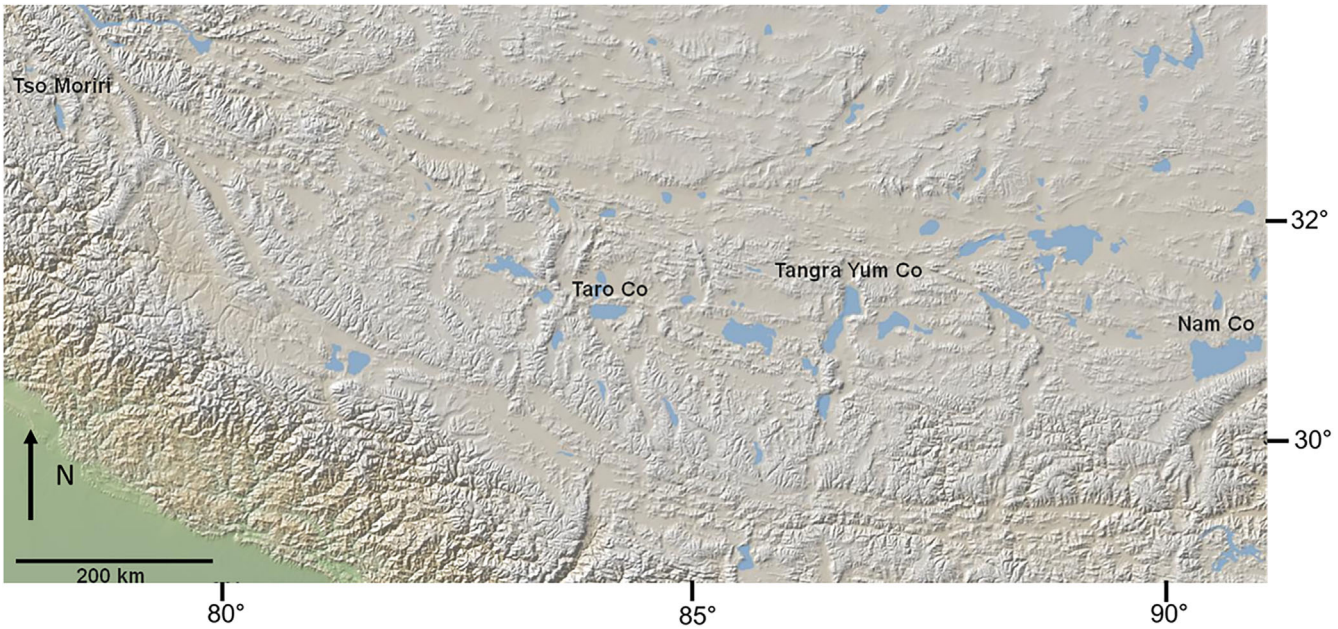

Figure 5. Location of the four lakes considered for the lake system comparison on the southern Tibetan Plateau.Source: www.geomapapp.org

last 0.5 cal ka BP is recorded. The lake level possibly rose slightly earlier than previously reported by Ahlborn *et al.* (2016), also given the chronology's uncertainty (±0.3 ka).

As Ahlborn *et al.* (2017) reported, we also note the first synchronous development between 17 and 16 ka where relatively low lake level conditions switch with the start of deglaciation to an increasing lake level registered in Taro Co (Alivernini *et al.*, 2018), Nam Co (Kasper *et al.*, 2015) and Tso Moriri (Mishra *et al.*, 2015) along an east–west transect on the Tibetan Plateau (Fig. 5).

After this shift, between 12 and 8.5 ka, an increase in moisture availability and temperature at the transition to the Holocene and a general precipitation decrease thereafter is reported for Taro Co (Alivernini *et al.*, 2018), Tso Moriri (Mishra *et al.*, 2015) and Nam Co (Kasper *et al.*, 2015), showing a similar pattern with Tangra Yumco. A lowstand recorded around 2 ka ago followed by an increase in lake level was also reported by Kasper *et al.* (2015) for Nam Co to the east and by Alivernini *et al.* (2018) for Taro Co to the west. For lake Tso Moriri, Leipe *et al.* (2014) registered, during the general trend of decreasing humidity after 9 ka, an increase in moisture availability between 1.1 and 0.4 ka. Considering the uncertainties of the chronological model for the Tso Moriri core (Leipe *et al.*, 2014) and the time lag for this event when comparing the two records we assume a possible synchronous timing. This last sequence is probably related to minor variations of the monsoonal components in the lakes studied (Kasper *et al.*, 2012; Ahlborn *et al.*, 2016).

Conclusions

According to the ostracod-based approach used here and the comparison with other datasets, the lake level evolution of the Tangra Yumco lake system as refined with the ostracod-based transfer function and the $\delta^{18}O$ analysis can be divided into six main phases.

- In the oldest stage (17–10.5 ka) conductivity and $\delta^{18}O$ generally decrease from relatively high values, in phase with the general increasing levels of the other considered Tibetan lakes.
- At around 10 ka, a decrease of conductivity in contrast to Ahlborn *et al.*'s (2016) curve is recorded. The different trend in the ostracod-based transfer function can be explained by a switch from an open to a closed lake basin and a mix of saltier water from Tangqung Co with oligohaline water from Tangra Yumco.
- Between 9.8 and 7.5 cal ka BP the ostracod fauna and conductivity based on it indicate a slow and progressive lowering of the lake level. This trend is also confirmed by $\delta^{18}O$ analysis.
- During the period 7.5–3.7 cal ka BP the general lack of data for both for the ostracod dataset and for the OSL samples does not allow a more precise reconstruction, although the moderate trend of increasing of $\delta^{18}O$ could be related to a decrease of the lake level.
- After this, the conductivity is in general in good agreement with Ahlborn *et al.*'s (2016) lake level curve, especially around 2 ka, where the fast switch of decreasing and later increasing lake level is synchronously mirrored by the conductivity curve.
- Thereafter, the conductivity, $\delta^{18}O$ and lake level curve agree until 0.4 ka, where the conductivity starts to decrease earlier than the rise of the lake level and the positive shift of the $\delta^{18}O$.

Comparison of the evolution of the Tangra Yumco lake system with the adjacent basins along an east–west transect shows synchronism for almost all the events recognizable at Tangra Yumco. However, the ostracod-based transfer function has proven to be a valuable tool for refining lake level curves, discriminating climatic and hydrographic effects such as switching between closed and open lakes.

Acknowledgements. We thank our colleagues from ITP-CAS, TU Braunschweig and FSU Jena for their support during fieldwork at Tangra Yumco. The present study was funded by the German Research Foundation under DFG grant FR1489/4 within the Priority Program SPP 1372 TiP 'Tibetan Plateau: Formation – Climate – Ecosystems' and by a Graduate Scholarship of Thuringia.

Abbreviation. OSL, optically stimulated luminescence.

References

Ahlborn M, Haberzettl T, Wang J *et al.* 2015. Sediment dynamics and hydrologic events affecting small lacustrine systems on the southern-central Tibetan Plateau – the example of TT Lake. *The Holocene* **25**: 508–522.

Ahlborn M, Haberzettl T, Wang J *et al.* 2016. Holocene lake level history of the Tangra Yumco lake system, southern-central Tibetan Plateau. *The Holocene* **26**: 176–187.

Ahlborn M, Haberzettl T, Wang J *et al.* 2017. Synchronous pattern of moisture availability on the southern Tibetan Plateau since 17.5 cal. ka BP – the Tangra Yumco lake sediment record. *Boreas* **46**: 229–241.

Akita LG, Frenzel P, Wang J *et al.* 2016. Spatial distribution and ecology of the Recent Ostracoda from Tangra Yumco and adjacent waters on the southern Tibetan Plateau: A key to palaeoenvironmental reconstruction. *Limnologica* **59**: 21–43.

Akita LG, Frenzel P, Haberzettl T *et al.* 2015. Ostracoda (Crustacea) as indicators of subaqueous mass movements: an example from the large brackish lake Tangra Yumco on the southern Tibetan Plateau, China. *Palaeogeography, Palaeoclimatology, Palaeoecology* **419**: 60–74.

Alivernini M, Lai Z, Frenzel P *et al.* 2018. Late Quaternary lake level changes of Taro Co and neighbouring lakes, Southwestern Tibetan Plateau, based on OSL dating and ostracod analysis. *Global and Planetary Change* **166**: 1–18.

Armijo R, Tapponnier P, Mercier JL *et al.* 1986. Quaternary extension in southern Tibet: field observations and tectonic implications. *Journal of Geophysical Research* **91**: 13803–13872.

Biskop S, Maussion F, Krause P *et al.* 2015. What are the key drivers of regional differences in the water balance on the Tibetan Plateau? *Hydrology and Earth System Sciences Discussions* **12**: 4271–4314.

Boomer I, Wünnemann B, Mackay AW *et al.* 2009. Advances in understanding the Late Holocene history of the Aral Sea region. *Quaternary International* **194**: 79–90.

Frenzel P, Wrozyna C, Xie M *et al.* 2010. Palaeo-water depth estimation for a 600-year record from Nam Co (Tibet) using an ostracod-based transfer function. *Quaternary International* **218**: 157–165.

Galy A, France-Lanord C. 1999. Weathering processes in the Ganges-Brahmaputra basin and the riverine alkalinity budget. *Chemical Geology* **159**: 31–60.

Gao JB, Li SC, Zhao ZQ. 2010. Validating the demarcation of eco-geographical regions: a geostatistical application. *Environmental Earth Sciences* **59**: 1327–1336.

Günther F, Aichner B, Siegwolf R *et al.* 2013. A synthesis of hydrogen isotope variability and its hydrological significance at the Qinghai-Tibetan Plateau. *Quaternary International* **313–314**: 3–16.

Günther F, Thiele A, Biskop S *et al.* 2016. Late Quaternary hydrological changes at Tangra Yumco, Tibetan Plateau: a compound-specific isotope-based quantification of lake level changes. *Journal of Paleolimnology* **55**: 369–382.

Günther F, Witt R, Schouten S *et al.* 2015. Quaternary ecological responses and impacts of the Indian Ocean Summer Monsoon at Nam Co, Southern Tibetan Plateau. *Quaternary Science Reviews* **112**: 66–77.

Guo Y, Zhu L, Frenzel P *et al.* 2016. Holocene lake level fluctuations and environmental changes at Taro Co, southwestern Tibet, based on ostracod-inferred water depth reconstruction. *The Holocene* **26**: 29–43.

Haberzettl T, Henkel K, Kasper T *et al.* 2015. Independently dated paleomagnetic secular variation records from the Tibetan Plateau. *Earth and Planetary Science Letters* **416**: 98–108.

Henkel K, Haberzettl T, St-Onge G *et al.* 2016. High-resolution paleomagnetic and sedimentological investigations on the Tibetan Plateau for the past 16 ka cal B.P. —The Tangra Yumco record. *Geochemistry, Geophysics, Geosystems* **17**: 774–790.

Juggins S 2003. User Guide C2, Software for Ecological and Palaeoecological Data Analysis and Visualisation, User Guide Version 1.3. Newcastle upon Tyne: Department of Geography, University of Newcastle.

Kasper T, Haberzettl T, Doberschütz S *et al.* 2012. Indian Ocean Summer Monsoon (IOSM)-dynamics within the past 4 ka recorded in the sediments of Lake Nam Co, central Tibetan Plateau (China). *Quaternary Science Reviews* **39**: 73–85.

Kasper T, Haberzettl T, Wang J *et al.* 2015. Hydrological variations on the Central Tibetan Plateau since the Last Glacial Maximum and their teleconnection to inter-regional and hemispheric climate variations. *Journal of Quaternary Science* **30**: 70–78.

Kong P, Na C, Brown R *et al.* 2011. Cosmogenic ^{10}Be and ^{26}Al dating of paleolake shorelines in Tibet. *Journal of Asian Earth Sciences* **41**: 263–273 [DOI: 10.1016/j.jseaes.2011.02.016].

Kropáček J, Maussion F, Chen F *et al.* 2013. Analysis of ice phenology of lakes on the Tibetan Plateau from MODIS data. *Cryosphere* **7**: 287–301.

Leipe C, Demske D, Tarasov PE. 2014. A Holocene pollen record from the northwestern Himalayan lake Tso Moriri: implications for palaeoclimatic and archaeological research. *Quaternary International* **348**: 93–112.

Leng MJ, Marshall JD. 2004. Palaeoclimate interpretation of stable isotope data from lake sediment archives. *Quaternary Science Reviews* **23**: 811–831.

Liu XJ, Lai ZP, Zeng FM *et al.* 2013. Holocene lake level variations on the Qinghai-Tibetan Plateau. *International Journal of Earth Sciences* **102**: 2007–2016.

Long H, Lai Z, Frenzel P *et al.* 2012. Holocene moist period recorded by the chronostratigraphy of a lake sedimentary sequence from Lake Tangra Yumco on the south Tibetan Plateau. *Quaternary Geochronology* **10**: 136–142.

Maussion F, Scherer D, Mölg T *et al.* 2014. Precipitation seasonality and variability over the Tibetan Plateau as resolved by the high Asia reanalysis. *Journal of Climate* **27**: 1910–1927.

Miehe S, Miehe G, van Leeuwen JFN *et al.* 2014. Persistence of Artemisia steppe in the Tangra Yumco Basin, west-central Tibet, China: despite or in consequence of Holocene lake-level changes? *Journal of Paleolimnology* **51**: 267–285.

Mischke S. 2012. Quaternary ostracods from the Tibetan Plateau and their significance for environmental and climate-change studies. In: *Ostracoda as Proxies for Quaternary Climate Change*, Horne DJ, Holmes J, Rodriguez-Lazaro J, Viehberg F (eds). *Developments in Quaternary Science* **17**: 263–279.

Mischke S, Herzschuh U, Massmann G *et al.* 2007. An ostracod-conductivity transfer function for Tibetan lakes. *Journal of Paleolimnology* **38**: 509–524.

Mischke S, Herzschuh U, Sun Z *et al.* 2006. Middle Pleistocene Ostracoda from a large freshwater lake in the presently dry Qaidam basin (NW China). *Journal of Micropalaeontology* **25**: 57–64.

Mischke S, Zhang C. 2010. Holocene cold events on the Tibetan Plateau. *Global and Planetary Change* **72**: 155–163.

Mishra PK, Anoop A, Schettler G *et al.* 2015. Reconstructed late Quaternary hydrological changes from Lake Tso Moriri, NW Himalaya. *Quaternary International* **371**: 76–86.

Peng P, Zhu L, Guo Y *et al.* 2016 *2016 Ostracod-Inferred Conductivity Transfer Function and Its Utility in Palaeoconductivity Reconstruction in Tibetan Lakes*. American Geophysical Union: San Francisco, GC21H- 1195.

Rades EF, Hetzel R, Xu Q *et al.* 2013. Constraining Holocene lake-level highstands on the Tibetan Plateau by ^{10}Be exposure dating: a case study at Tangra Yumco, southern Tibet. *Quaternary Science Reviews* **82**: 68–77.

Rades EF, Tsukamoto S, Frechen M *et al.* 2015. A lake-level chronology based on feldspar luminescence dating of beach ridges at Tangra Yumco (southern Tibet). *Quaternary Research* **83**: 469–478.

Viehberg FA, Mesquita-Joanes F. 2012. Quantitative transfer function approaches in palaeoclimatic reconstruction using Quaternary ostracods. In: *Ostracoda as Proxies for Quaternary Climate Change*, Horne DJ, Holmes J, Rodriguez-Lazaro J, Viehberg F (eds). *Developments in Quaternary Science* **17**: 47–64.

Wang J, Peng P, Ma Q *et al.* 2010. Modern limnological features of Tangra Yumco and Zhari Namco. Tibetan Plateau. *Journal of Lake Sciences* **22**: 629–632 (in Chinese with English abstract).

Wrozyna C, Frenzel P, Daut G *et al.* 2012. Holocene lake-level changes of Lake Nam Co, Tibetan Plateau, deduced from ostracod assemblages and δ^{18}O and δ^{13}C signatures of their Valves. *Developments in Quaternary Sciences*. In: Ostracoda as Proxies for Quaternary Climate Change, Horne DJ, Holmes J, Rodriguez-Lazaro J, Viehberg F (eds). *Developments in Quaternary Science* **17**: 281–295.

Wrozyna C, Frenzel P, Steeb P *et al.* 2010. Stable isotope and ostracode species assemblage evidence for lake level changes of Nam Co, southern Tibet, during the past 600 years. *Quaternary International* **212**: 2–13.

Zhang Q. 2000. Uplift and environmental changes of the Tibetan Plateau. In *Mountain Geoecology and Sustainable Development of the Tibetan Plateau*, Zheng D, Zhang Q (eds). Kluwer Academic Publishers: Dordrecht; 19–55.

Zhu DG, Meng XG, Zhao XT *et al.* 2004. *On the Quaternary Environmental Evolution of the Nam Co Area, Tibet*. Geology Press: Beijing.